Burdenko's Journal of Neurosurgery
2026, No. 4, pp. 7–13
https://doi.org/10.17116/neiro2026900317

Phosphorus MR spectroscopy: energetic metabolism and Warburg effect

© N.E. Elagina, A.N. Tyurina, L.M. Fadeeva, G.V. Pavlova, A.V. Kosyrkova, I.N. Pronin

Burdenko Neurosurgery Center, Moscow, Russia

ABSTRACT

Magnetic resonance spectroscopy (MRS) is a complementary imaging technique enabling non-invasive metabolic characterization of tissues in clinical practice. Proton MRS is more common for analysis of metabolites such as lactate and choline. This is valuable for preoperative assessment of glioma grade. However, it does not directly reflect phosphate energy metabolism. Phosphorus MRS enables assessment of phosphorus-containing compounds involved in tumor energy metabolism and membrane turnover.

Objective. To assess the role of phosphorus MRS in metabolic characterization of low-grade and high-grade gliomas.

Material and methods. The study included 46 patients with gliomas: 31 patients with high-grade gliomas and 15 patients with low-grade gliomas. The control group comprised 15 healthy volunteers. All participants underwent phosphorus MRS with assessment of spectral parameters of phosphorus-containing metabolites, metabolic ratios and intracellular pH.

Results. Phosphorus MRS revealed differences in metabolic profile of tumor tissue between high-grade and low-grade gliomas. High-grade gliomas were characterized by signs of impaired energy and membrane metabolism, including changes in phosphorus-containing metabolite ratios and shift in intracellular pH. Low-grade gliomas demonstrated less severe metabolic alterations.

Conclusion. Phosphorus MRS is a promising complementary imaging modality for non-invasive assessment of metabolic features of gliomas. This method may be used to refine their biological characteristics at the preoperative stage.

Keywords: *phosphorus MR spectroscopy, low-grade glioma, high-grade glioma, energy metabolism.*

INFORMATION ABOUT THE AUTHORS:
Elagina N.E. — https://orcid.org/0000-0002-9793-5376
Tyurina A.N. — https://orcid.org/0000-0002-2333-7867
Fadeeva L.M. — https://orcid.org/0000-0002-3240-5585
Pavlova G.V. — https://orcid.org/0000-0002-6885-6601
Kosyrkova A.V. — https://orcid.org/0000-0002-3019-5203
Pronin I.N. — https://orcid.org/0000-0002-4480-0275
Corresponding author: Elagina N.E. — e-mail: hope.11@bk.ru

TO CITE THIS ARTICLE:
Elagina NE, Tyurina AN, Fadeeva LM, Pavlova GV, Kosyrkova AV, Pronin IN. Phosphorus MR spectroscopy: energetic metabolism and Warburg effect. *Burdenko's Journal of Neurosergery*. 2026;90(4):7–13. (In Russ.). https://doi.org/10.17116/neiro2026900417

Introduction

The Warburg effect is a metabolic reorganization phenomenon in tumor cells, when they preferentially utilize anaerobic glycolysis for energy despite sufficient oxygen. Normally, adenosine triphosphate (ATP) is primarily released in mitochondria through oxidative phosphorylation (approximately 36 ATP molecules from a glucose molecule) with only a small part released through anaerobic glycolysis. However, malignant cells predominantly convert glucose into lactate regardless of available oxygen and produce only ~4 ATP molecules per a glucose molecule. The Warburg effect is a typical feature of many malignancies, including aggressive brain gliomas such as glioblastoma. Glucose uptake correlates with tumor aggressiveness. High-grade gliomas (HGG) are characterized by higher glucose metabolism and intense capture of ^{18}F-fluorodeoxyglucose. Slow-growing low-grade gliomas (LGG) typically demonstrate moderate metabolism [1]. Accelerated glycolysis in tumors is accompanied by «reverse pH gradient». Indeed, extracellular environment becomes acidic due to lactate accumulation, while alkaline pH is maintained inside cells. This shifted intracellular pH promotes tumor cell proliferation. It is one of the hallmarks of the Warburg effect. In general, the Warburg effect is a typical feature of malignant tumors and associated with their aggressiveness [2].

Various neuroimaging methods are used for non-invasive research of glioma metabolism. PET/CT with ^{18}F-fluorodeoxyglucose is the most common method for assessing glucose consumption in tumors [3]. Proton magnetic resonance spectroscopy (^{1}H MRS) provides information on metabolites such as lactate (marker of anaerobic glycolysis) and total choline (marker of membrane exchange). These data are valuable to distinguish HGG (with high lactate and choline peaks) and LGG. In addition, ^{1}H MRS can facilitate non-invasive assessment of tumor IDH status, since 2-hydroxyglutarate can be detect-

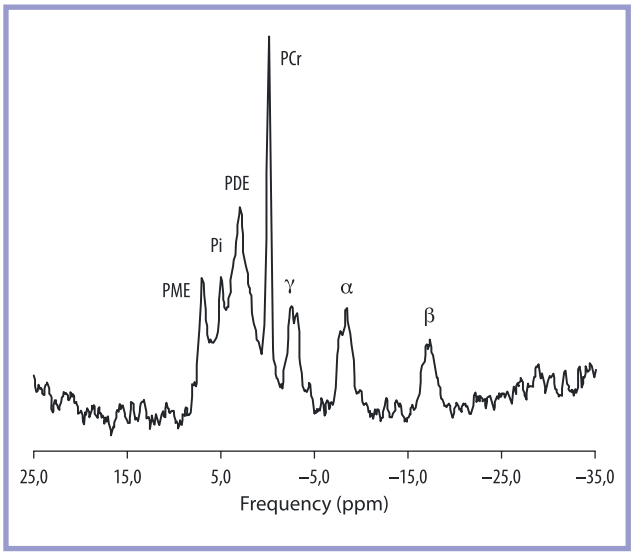


Fig. 1. **Phosphorus spectrum of the brain in a healthy volunteer indicating peaks of metabolites: phosphocreatine (PCr), inorganic phosphate (Pi), phosphomonoesters (PME), phosphodiesters (PDE), as well as α-, β- and γ-fractions of adenosine triphosphate (ATP).**

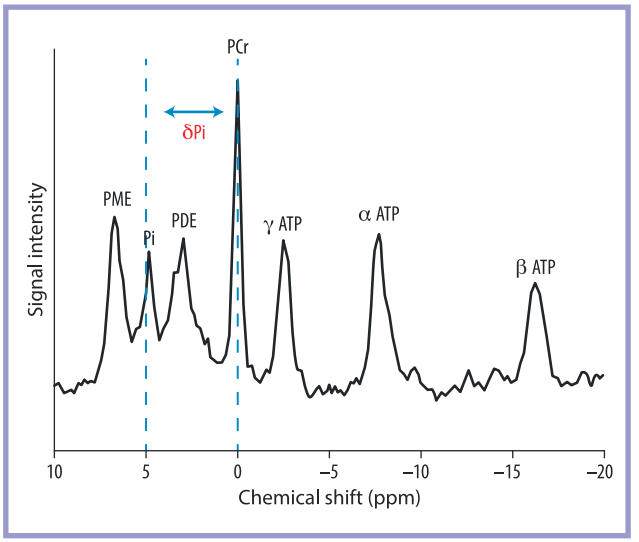


Fig. 2. **Calculation of intracellular pH based on chemical shift of inorganic phosphate (Pi) relative to phosphocreatine peak (PCr).**

ed in IDH-mutant gliomas. It is a specific oncometabolite associated with this molecular genetic rearrangement [4]. However, ^{1}H MRS does not allow direct measurement of energy phosphates or differentiation of certain phosphometabolites of membrane exchange. In this regard, phosphorus MR spectroscopy (31P MRS) is of particular value.

^{31}P MRS is based on recording radiofrequency signal from phosphorus nuclei in biologically important phosphorus compounds. In clinical practice, ^{31}P MRS is performed on at least 3.0 T MR scanners (less commonly 7.0 T) using specialized dual radiofrequency coils (^{1}H/31P). Unlike ^{1}H MRS, ^{31}P MRS requires special setup and calibration, as phosphorus concentration in tissues is many times lower than concentration of protons. In final spectrum, we can distinguish 7 main signal groups corresponding to various metabolites **(Fig. 1)**:

1. Phosphocreatine (PCr) is the highest peak at 0 ppm. PCr serves as an energy-intensive buffer in cells and maintains ATP through reaction with creatine kinase. In intact brain tissue, PCr is present in high concentrations, especially in gray matter, ensuring rapid ATP re-synthesis.
2. Inorganic phosphate (Pi) is a peak at ~ +5 ppm. Its position depends on pH. Chemical shift of Pi relative to PCr is used to calculate intracellular pH.
3. Phosphomonoesters (PME) are a group of metabolites at +6—7 ppm, including phospholipid precursors, primarily phosphocholine and phosphoethanolamine. PME characterize intensity of cell membrane synthesis and activity of phospholipid biosynthetic pathways.
4. Phosphodiesters (PDE) are peaks at +2—3 ppm, corresponding to phospholipid breakdown products, primarily glycerophosphocholine and glycerophosphoethanolamine. PDEs are a marker of membrane catabolism.
5. Adenosine triphosphate (ATP) has three resonance peaks from ~ –2 to –16 ppm from α-, β- and γ-phosphate groups of ATP molecule. ATP is the main energy carrier, and its level characterizes cellular energy status [5].

The objective of the study was to analyze metabolic status of gliomas using phosphorus MRS, tissue pH and Warburg effect in various gliomas.

Material and methods

The study included 46 patients aged 23—67 years with MR-verified primary supratentorial brain glioma. All patients underwent resection followed by histological assessment according to the 2021 WHO classification [6]. The control group consisted of 15 healthy volunteers.

There were 15 patients with LGG (WHO Grade II) and 31 ones with HGG including 11 patients with WHO Grade III tumors (astrocytoma — 9, oligodendroglioma — 2) and 20 with WHO Grade IV neoplasms (astrocytoma — 1, glioblastoma — 19).

We used 3.0 T MR scanner with dual ^{1}H/^{31}P coil and appropriate protocol (T1WI, T2WI, T1+Gd (with contrast enhancement) and 31P MRS). In our study, the region of interest (ROI) was defined using axial T2WIs. The ROI included lesion and minimal amount of intact tissue. Signals from tissues outside the ROI were suppressed by defining pre-saturation regions. To improve magnetic field homogeneity within the ROI, we applied high-order shimming at hydrogen frequency (128 MHz). The coil parameters were adjusted at phosphorus frequency (51.7 MHz) according to phosphocreatine peak. MRS was then performed (scanner setup time — 20 min, data acquisition time — 12 min). Post-processing of data was performed in SAGE software (Spectroscopy Analysis

Table 1. **Median chemical shifts (relative to phosphocreatine) of the main metabolites of phosphorus spectrum in different groups.**

Metabolites	Median, ppm							
	n	PME	Pi	PDE	PCr	ATP		
						γ	α	β
Control group	15	–6.800	–4.722	–2.975	0	2.645	7.485	16.126
LGG	15	–6.824	–4.746	–2.881	0.000	2.503	7.556	16.138
HGG	31	–6.824	–4.746	–2.881	0.000	2.585	7.532	16.221

Distribution of metabolites depending on area under peak and amplitude is presented in **Fig. 3, 4.**

by General Electric; GE Medical Systems, USA) with quantitative analysis of metabolite.

In addition to detection of phosphorus-containing metabolites, ^{31}P MRS provides a unique opportunity to assess cellular biophysical parameters, particularly intracellular acidity (pH).

Tissue (intracellular) pH was calculated using the formula obtained by Petroff O.A. et al. [7]:

$$pH=6.77+\log[(\delta Pi-3.29)/(5.68-\delta Pi)],$$

where dPi is a chemical shift of inorganic phosphate relative to phosphocreatine peak **(Fig. 2)**.

Analysis of pH is diagnostically important. Indeed, intracellular alkalosis indicates malignant transformation. Normal cells tend to become acidic under hypoxia, while cancer cells maintain neutral-alkaline pH. Furthermore, pH influences the effectiveness of chemo- and radiotherapy (acidic environment weakens the effect of some alkylating agents and increases sensitivity to radiotherapy). Therefore, noninvasive measurement of tumor pH is valuable for treatment strategy. For example, lower pH of tumor (<7.0) can indicate a tendency towards necrosis and potentially higher sensitivity to radiotherapy, while higher pH (~7.2—7.4) indicates aggressive metabolism and, possibly, the need for more intensive therapy.

Results

Mean age of patients with HGG was 48.9±10.9 years (median 51, range 23—67). In the LGG group, these parameters differed significantly: mean age was 36.1±9.5 years (median 35, range 25—64). Age of people in the control group was significantly lower (mean 25.5±1.5, median 25, range 23—28).

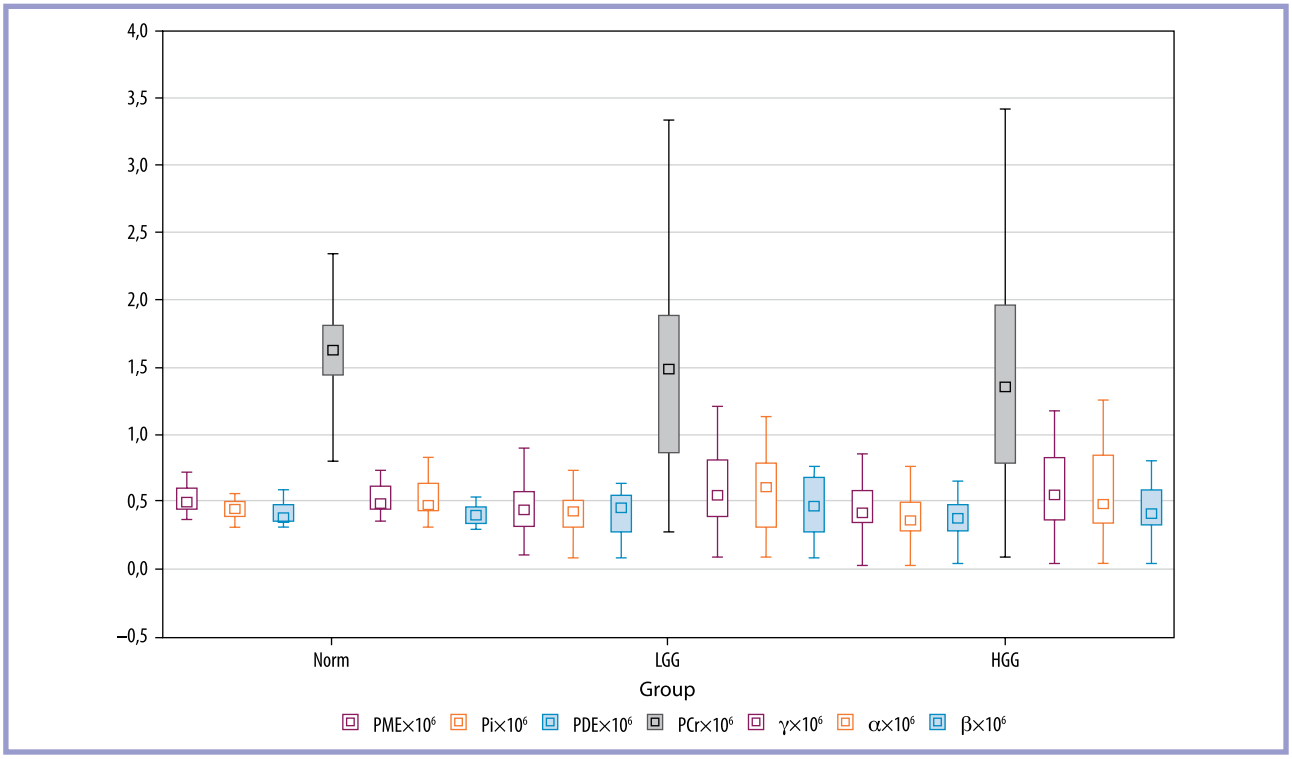


Fig. 3. **Metabolite concentrations depending on area under peaks of phosphorus spectrum in all groups.**

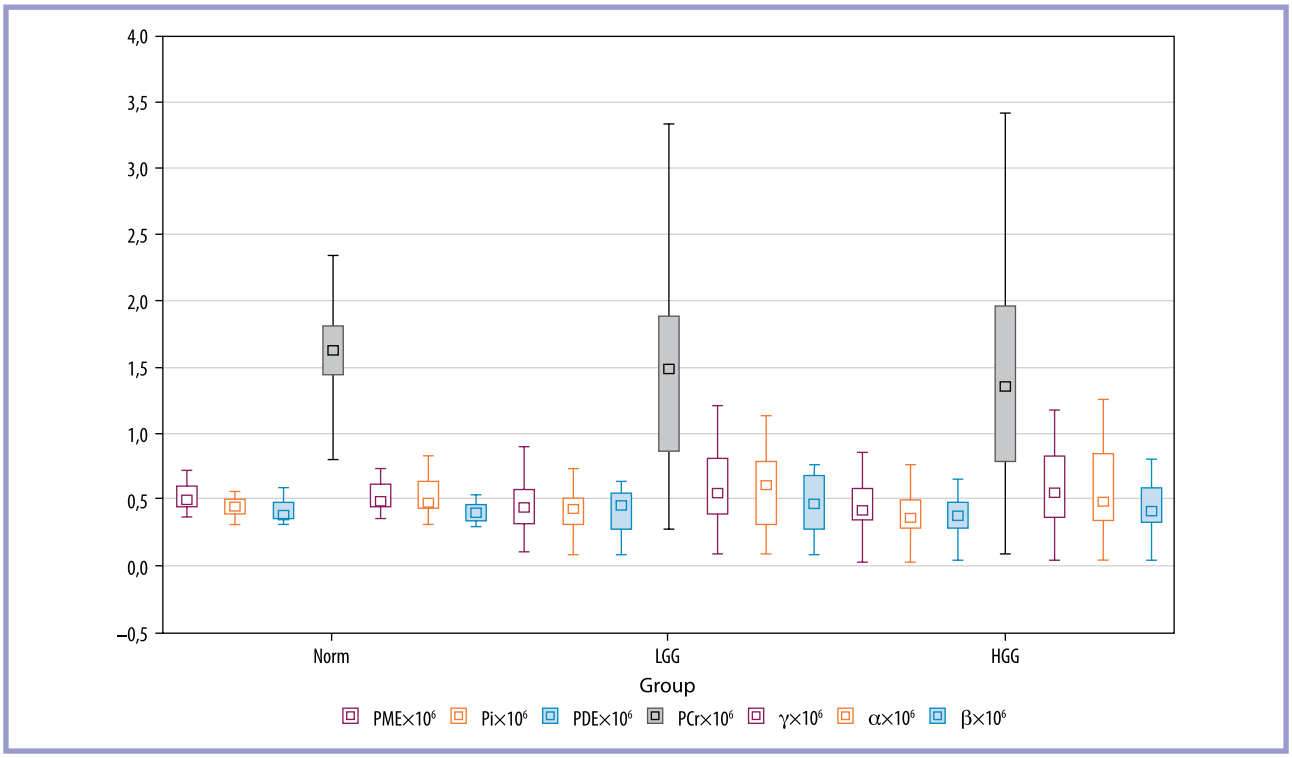


Fig. 4. **Metabolite concentrations depending on peak amplitude of phosphorus spectrum in all groups.**

In all cases, we obtained spectra that allowed identification of the main peaks: PME, Pi, PDE, PCr, as well as three ATP components (γ, α, β). Chemical shifts of resonances were stable in all groups that confirmed correct settings and comparability of data **(Table)**.

The Kruskal-Wallis test revealed significant differences between three groups only for the following absolute characteristics of energy metabolites:

— total ATP level (γ, α, β) (p=0.0391);
— β-ATP peak amplitude (p=0.0165);
— γ-ATP peak amplitude (p=0.0031);
— α-ATP peak amplitude has no significant between-group differences (p>0.5).

Thus, these parameters significantly characterize differences in tissue energy status when comparing normal and tumor tissue.

We analyzed many relative parameters and found the following significant (Mann—Whitney test) variables after comparison of control group and patients with HGG **(Fig. 5)**:

— PME/α-ATP, p=0.000572;
— α-ATP/Pi, p=0.015799;
— β-ATP/Pi, p=0.003399.

These differences indicate disruption of energy balance and altered membrane metabolism in malignant tumors.

Among healthy volunteers and patients with LGG, significant differences were found for the following variables:

— PME/α-ATP, p=0.000174;
— PCr/α-ATP, p=0.003155;
— α-ATP/Pi, p=0.005704;
— β-ATP/Pi, p=0.002702.

This demonstrates sensitivity of 31P MRS to even moderate metabolic changes in LGGs.

Measurement of intracellular pH found no significant increase in gliomas. However, this parameter was highly variable in patients with gliomas. Significant difference was observed not in pH, but in coefficient of variation (F-test: p<0.0001) **(Fig. 6)**.

Reduced phosphocreatine and increased Pi/ATP ratio in HGG demonstrate ATP re-synthesis system overload. We found no significant changes in PCr, but ATP/Pi ratios differed significantly between tumor and normal tissue. This indicates that glioma cells are essentially in a state of chronic «energy deficit» and maintain survival through the Warburg effect.

Discussion

According to the literature, the Warburg effect is closely related to histological grading of gliomas. HGGs are in a state of increased metabolic stress and adapt through anaerobic glycolysis. MR scan of a patient with HGG is presented in **Fig. 7**.

Increased PME is associated with enhanced synthesis of membranes and active cell proliferation (since phosphocholine is involved in biosynthesis of cell membranes). In intact brain tissue, total PME signal is relatively low, whereas it increases proportionally to malignancy grade in tumors. The PME/α-ATP ratio indicates relative accumulation of PMEs in tumor under reduced concentra-

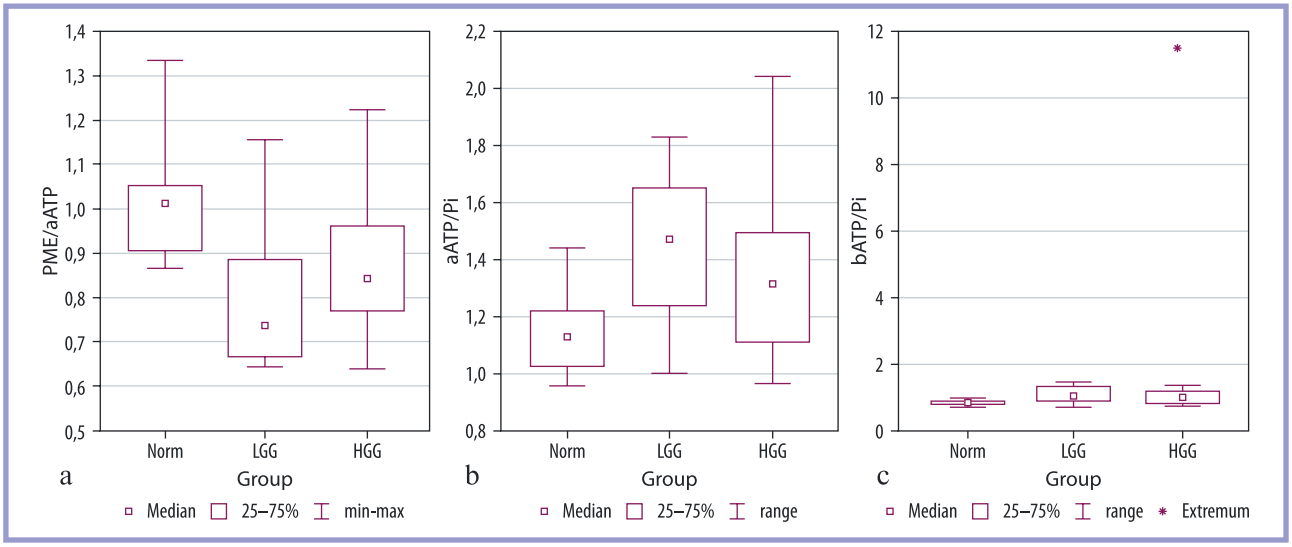


Fig. 5. **Between-group differences in metabolic ratios according to phosphorus MRS.**
PME/α-ATP (a), α-ATP/Pi (b) and β-ATP/Pi (c) between patients with gliomas and the control group. Significant differences ($p<0.05$) were observed when comparing HGG and LGG with the control group.

tion of high-energy phosphates. This indicator is a marker of enhanced membrane synthesis associated with tumor cell proliferation.

Mild decrease in β- and γ-ATP (nucleoside triphosphates). In glioma tissue, we found no significant decrease in amplitude of β- and γ-ATP fractions compared to normal brain tissue. This may be due to small sample size and technical limitations of spectroscopy (large voxel). Thus, further researches are required.

According to some data, decrease in β- and γ-ATP is most pronounced in HGG. This is consistent with higher energy demand and rapid depletion of resources in highly malignant cells. Some data indicate that ATP in metastatic brain tumors may decline even more significantly than in gliomas. This is consistent with frequent necrosis of metastatic tumors [8].

Increased Pi/ATP ratio in tumor tissue reflects higher energy exchange. We found significant difference in α-ATP/Pi and β-ATP/Pi ratios between patients with gliomas and the control group. Tumors are characterized by reduced β- and α-ATP, as well as a tendency towards Pi accumulation. This is associated with ATP hydrolysis and PCr breakdown under energy deficiency. The Pi/ATP ratio is an indicator of ATP exchange rate. Thus, increased Pi under decreased PCr and ATP indicates the Warburg effect (intensive anaerobic metabolism with accumulation of phosphagen breakdown products) [2].

Chemical shift of Pi estimates mean intracellular pH. Intracellular pH of normal brain is ~6.99—7.0, in tumors — 7.1—7.2 [7]. Petroff O.A. et al. [7] described significantly higher pH in brain tumors compared to the control group (7.12±0.10 vs. 7.04±0.06). Alkaline intracellular environment is especially clear in highly malignant gliomas. This fact is fully consistent with the Warburg effect and active expression of proton pumps and lactate transporters maintaining intracellular pH favorable for oncogenic metabolism. Paech D. et al. [9] confirmed these data. The authors used an ultra-high-field MR scanner (7.0 T) and demonstrated intracellular pH increase throughout tumor volume and its relationship with Ki-67 index. We have previously demonstrated intracellular pH increase in glioblastoma cells compared to normal brain tissue. This parameter was suggested to be a potential early marker of metabolic disorders inaccessible to standard MRI [10]. These results are consistent with the concept of the Warburg effect and «reverse pH gradient» phenomenon (acidic extracellular environment of tumor due to lactate accumulation and relative intracellular alkalization). In the present study, no significant between-group differences in mean pH were found. However, HGGs were characterized by significantly higher pH variation coefficient compared to LGG and control group ($p<0.0001$) **(Fig. 6)**. This fact may indicate metabolic heterogeneity of HGG. According to the literature, different areas of the same glioblastoma may have opposite pH profiles. For example, contrast-enhanced areas are more alkaline, while perifocal zone of abnormal signal is closer to normal [11].

In addition, approaches to spatially resolved quantitative MRS are being rapidly improved. Baboli M. et al. [12] demonstrated that whole-brain 3D MRS combined with EPTI improves accuracy of absolute quantification of metabolites in tumor tissue and infiltration zones. This emphasizes the role of metabolic mapping in analysis of glioma heterogeneity. New methodological studies demonstrate that multiparametric post-processing algorithms and their integration with CEST visualization and machine learning methods can increase accuracy of non-invasive pH mapping based on 31P MRS data [13, 14].

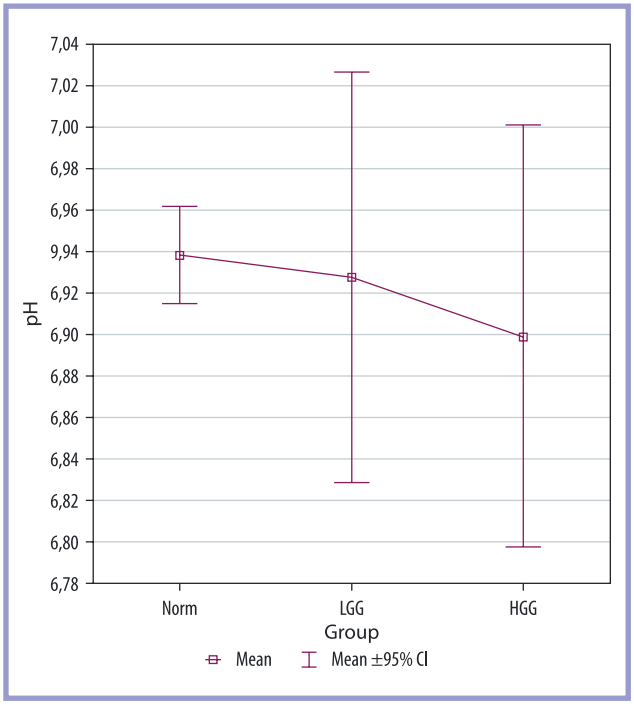


Fig. 6. **Variability of intracellular pH coefficient in the control group and patients with LGG and HGG (means and standard deviations).**

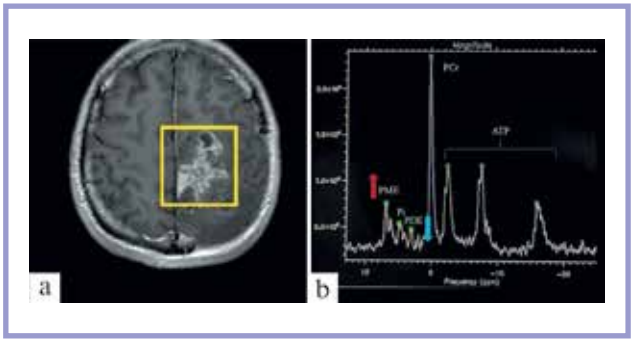


Fig. 7. **Phosphorus MRS in a patient with high-grade glioma.**
a — MR scan of a patient with high-grade glioma; the yellow square indicates the region of interest; b — phosphorus spectrum of the selected area; the red arrow indicates increase in PME, blue arrow — decrease in PDE.

Conclusion

Phosphorus MRS reveals differences in metabolic profile of tumor and normal brain tissue. Gliomas are characterized by decreased β- and γ-adenosine triphosphate, altered ratios of inorganic phosphate and phosphomonoesters to adenosine triphosphate, and highly variable intracellular pH, especially in high-grade gliomas. These changes reflect activation of anaerobic glycolysis, disruption of energy homeostasis and enhanced synthesis of cell membranes (key manifestations of the Warburg effect). Thus, phosphorus MRS may be used as noninvasive tool for quantifying metabolic reorganization in gliomas and complementing standard preoperative diagnostic methods.

This study was supported by the Ministry of Science and Higher Education of the Russian Federation (Agreement No. 075-15-2025-559 dated June 11, 2025).

Author contribution:
Concept and design of the study — Pronin I.N., Pavlova G.V., Kosyrkova A.V., Fadeeva L.M., Tyurina A.N., Elagina N.E.
Collection and analysis of data — Elagina N.E., Tyurina A.N., Fadeeva L.M.
Statistical analysis — Fadeeva L.M.
Writing the text — Elagina N.E., Tyurina A.N.
Editing — Pronin I.N., Fadeeva L.M.

No conflict of interests to declare.

REFERENCES

1. Liu P, Zeng YP, Qu H, Zheng WY, Zhou TX, Hang LF, Jiang GH. Multiparametric simultaneous hybrid 18F-fluorodeoxyglucose positron emission tomography/magnetic resonance imaging (18F-FDG PET/MRI) incorporating intratumoral and peritumoral regions for grading of glioma. *Quantitative Imaging in Medicine and Surgery.* 2024;14(8):5665-5681. https://doi.org/10.21037/qims-24-280
2. Liberti MV, Locasale JW. The Warburg Effect: How Does it Benefit Cancer Cells? *Trends in Biochemical Sciences.* 2016;41(3):211-218. https://doi.org/10.1016/j.tibs.2015.12.001
3. Hangel G, Schmitz-Abecassis B, Sollmann N, Pinto J, Arzanforoosh F, Barkhof F, Booth T, Calvo-Imirizaldu M, Cassia G, Chmelik M, Clement P, Ercan E, Fernández-Seara MA, Furtner J, Fuster-Garcia E, Grech-Sollars M, Guven NT, Hatay GH, Karami G, Keil VC, Kim M, Koekkoek JAF, Kukran S, Mancini L, Nechifor RE, Özcan A, Ozturk-Isik E, Piskin S, Schmainda KM, Svensson SF, Tseng CH, Unnikrishnan S, Vos F, Warnert E, Zhao MY, Jancalek R, Nunes T, Hirschler L, Smits M, Petr J, Emblem KE. Advanced MR Techniques for Preoperative Glioma Characterization: Part 2. *Journal of Magnetic Resonance Imaging.* 2023;57(6):1676-1695. https://doi.org/10.1002/jmri.28663
4. Tyurina AN, Batalov AI, Zakharova NE, Fadeeva LM, Kalaeva DB, Pronin IN. Non-invasive detection of IDH-1 mutation in brain gliomas based on proton MR spectroscopy. *I.P. Pavlov Journal of Higher Nervous Activity.* 2024;74(1):77-84. (In Russ.). https://doi.org/10.31857/S0044467724010088
5. Jett S, Boneu C, Zarate C, Carlton C, Kodancha V, Nerattini M, Battista M, Pahlajani S, Williams S, Dyke JP, Mosconi L. Systematic review of 31P-magnetic resonance spectroscopy studies of brain high energy phosphates and membrane phospholipids in aging and Alzheimer's disease. *Frontiers in Aging Neuroscience.* 2023;15:1183228. https://doi.org/10.3389/fnagi.2023.1183228
6. *WHO Classification of Tumours Editorial Board. Central nervous system tumours. 5th ed.* Lyon: International Agency for Research on Cancer; 2021.
7. Petroff OA, Prichard JW, Behar KL, Alger JR, den Hollander JA, Shulman RG. Cerebral intracellular pH by 31P nuclear magnetic resonance spectroscopy. *Neurology.* 1985;35(6):781-788. https://doi.org/10.1212/WNL.35.6.781
8. Kannan N, Sathyanathan BP. Evaluation of Metabolic Characteristics of Brain Tumours Utilising 31-Phosphorus MR Spectroscopy in 3T MRI: A Cross-sectional Study. *Journal of Clinical and Diagnostic Research.* 2025;19(1):TC01-TC06. https://doi.org/10.7860/JCDR/2025/67394.20491
9. Paech D, Weckesser N, Franke VL, Breitling J, Görke S, Deike-Hofmann K, Wick A, Scherer M, Unterberg A, Wick W, Bendszus M, Bachert P, Ladd ME, Schlemmer H-P, Korzowski A. Whole-Brain Intracellular pH Mapping of Gliomas Using High-Resolution 31P MR Spectroscopic Imaging at 7.0 T. *Radiology: Imaging Cancer.* 2024;6(1):e220127. https://doi.org/10.1148/rycan.220127
10. Mertsalova MP, Pronin IN, Zakharova NE, Podoprigora AE, Batalov AI, Tyurina AN, Shults EI, Pogosbekyan EL, Fadeeva LM, Golanov AV, Post-

nov AA, Rodionov PV. Intracellular pH measurement in glioblastoma cells: the possibilities of phosphorus-31 MR spectroscopy. *Burdenko's Journal of Neurosurgery.* 2020;84(6):26-32. (In Russ., In Engl). https://doi.org/10.17116/neiro20208406126

11. Franke VL, Breitling J, Boyd PS, Feignier A, Bangert R, Weckesser N, Schlemmer H-P, Ladd ME, Bachert P, Paech D, Korzowski A. A Versatile Look-Up Algorithm for Mapping pH Values and Magnesium Ion Content Using 31P MRSI. *NMR in Biomedicine.* 2024;37(6):e5113. https://doi.org/10.1002/nbm.5113
12. Baboli M, Wang F, Dong Z, Dietrich J, Uhlmann EJ, Batchelor TT, Cahill DP, Andronesi OC. Absolute Metabolite Quantification in Individuals with Glioma and Healthy Individuals Using Whole-Brain Three-dimensional MR Spectroscopic and Echo-planar Time-resolved Imaging. *Radiology.* 2024;312(3):e232401. https://doi.org/10.1148/radiol.232401
13. Schüre JR, Rajput J, Shrestha M, Deichmann R, Hattingen E, Maier A, Nagel AM, Dörfler A, Steidl E, Zaiss M. Toward Noninvasive High-Resolution In Vivo pH Mapping in Brain Tumors by 31P-Informed deepCEST MRI. *NMR in Biomedicine.* 2025;38(6):e70060. https://doi.org/10.1002/nbm.70060

Received 21.01.2026
Revised 19.03.2026
Accepted 07.05.2026

COMMENT

This manuscript addresses an important issue in neuroradiology and neurosurgery (the Warburg effect in gliomas as a biomarker of their malignancy). The authors used phosphorus spectroscopy to assess energy metabolism. Data from representative (n=46) and control groups are presented with appropriate statistical analysis. Conclusions appear logical and adequately reflect the objectives. Review includes articles over the recent years. The manuscript is distinguished by clear structure, completeness and logical presentation.

Konovalov R.N. (Moscow)